Why Is Remote Sensing of Amazon Forest Greenness So Challenging?

Arindam Samanta*

Department of Geography and Environment, Boston University, Boston, and Atmospheric and Environmental Research Inc., Lexington, Massachusetts

Sangram Ganguly

BAERI/NASA Ames Research Center, Moffett Field, California

Eric Vermote

Department of Geography, University of Maryland, College Park, College Park, Maryland

Ramakrishna R. Nemani

Biospheric Science Branch, NASA Ames Research Center, Moffett Field, California

Ranga B. Myneni

Department of Geography and Environment, Boston University, Boston, Massachusetts

Received 23 January 2012; accepted 24 March 2012

ABSTRACT: The prevalence of clouds and aerosols and their impact on satellite-measured greenness levels of forests in southern and central Amazonia are explored in this article using 10 years of NASA Moderate Resolution Imaging Spectroradiometer (MODIS) greenness data: normalized difference vegetation index (NDVI) and enhanced vegetation index (EVI). During the wet season (October–March), cloud contamination of greenness data is pervasive;

* Corresponding author address: Arindam Samanta, Atmospheric and Environmental Research Inc., 131 Hartwell Avenue, Lexington, MA 02421.
E-mail address: arindam.sam@gmail.com

DOI: 10.1175/2012EI440.1

nearly the entire region lacks uncorrupted observations. Even in the dry season (July–September), nearly 60%–66% of greenness data are corrupted, mainly because of biomass burning aerosol contamination. Under these conditions, spectrally varying residual atmospheric effects in surface reflectance data introduce artifacts into greenness indices; NDVI is known to artificially decrease, whereas EVI, given its formulation and use of blue channel surface reflectance data, shows artificial enhancement, which manifests as large patches of enhanced greenness. These issues render remote sensing of Amazon forest greenness a challenging task.

KEYWORDS: Amazon forests; Greenness; Vegetation index; Remote sensing

1. Introduction

Vegetation indices (VIs) are radiometric measures of photosynthetically active radiation absorbed by canopy chlorophyll and are therefore good surrogate measures of the physiologically functioning surface greenness level in a region (Myneni et al. 1995). The normalized difference vegetation index (Tucker 1979) of the National Oceanic and Atmospheric Administration (NOAA) Advanced Very High Resolution Radiometer (AVHRR) has been used effectively to analyze greenness changes at seasonal (Ferreira and Huete 2004) to interannual time scales (Asner et al. 2000; Gurgel and Ferreira 2003; Dessay et al. 2004) in the Amazon. The shortcomings of the AVHRR NDVI data—calibration degradation, loss of orbit, lack of satisfactory atmospheric correction, broad spectral bands, saturation in dense vegetation, insufficient validation, etc.—are for the most part remedied in the National Aeronautics and Space Administration (NASA) Moderate Resolution Imaging Spectroradiometer (MODIS) enhanced vegetation index (EVI) data (Justice et al. 1998; Vermote et al. 2002; Huete et al. 2002). Algorithm refinements through feedback from concerted validation efforts and multiple reprocessings of the growing MODIS data archive have led to progressively improved research-quality products ideally suited for studies of greenness dynamics in complex ecosystems such as the Amazon (e.g., Huete et al. 2006; Xiao et al. 2006; Myneni et al. 2007; Samanta et al. 2011a; Samanta et al. 2012; Xu et al. 2011).

Monitoring greenness of Amazon forests with satellite measurements is fraught with several pitfalls, the major being corruption from atmospheric effects leading to artificial changes in vegetation indices that are unrelated to any real changes on the ground. For example, Saleska et al. (Saleska et al. 2007) observed a greening anomaly in response to the 2005 drought, but this has been shown to be an artifact of atmospheric corruption of EVI and not observed in a later version of the same data (Samanta et al. 2010; Samanta et al. 2011b). This article is thus motivated by the need to comprehensively assess cloud and aerosol prevalence and corruption of greenness data, using a decade's worth of MODIS VI data.

2. Data

2.1. Greenness data: VI

These are satellite data-based measurements of vegetation greenness produced by NASA using blue [blue bidirectional reflectance factor (BRF_{BLUE}); 459–479 nm (nm)], red (BRF_{RED}; 620–670 nm) and near-infrared (NIR) (BRF_{NIR}; 842–876 nm)

band surface reflectance data from the MODIS instrument aboard the *Terra* and *Aqua* satellites (USGS 2011a; Huete et al. 2002). VIs consist of NDVI and EVI. NDVI is a radiometric measure of photosynthetically active radiation absorbed by canopy chlorophyll and therefore is a good surrogate measure of the physiologically functioning surface greenness level in a region (Myneni et al. 1995). NDVI has been used in many studies of vegetation dynamics in the Amazon (e.g., Asner et al. 2000; Dessay et al. 2004; Ferreira and Huete 2004). EVI is also a measure of greenness that generally correlates well with ground measurements of photosynthesis (e.g., Rahman et al. 2005; Sims et al. 2008) and found to be especially useful in high biomass tropical broadleaf forests like the Amazon (Huete et al. 2006). We used versions—also called collections—4 and 5 of *Terra* MODIS EVI data. Collection 5 (C5) is the latest version, superseding all previous versions.

The vegetation indices 16-day L3 global 1 km (MOD13A2) dataset contains VI at 1 km × 1 km spatial resolution and 16-day frequency. This 16-day frequency arises from compositing: that is, assigning one best-quality EVI value to represent a 16-day period. This dataset is available in tiles (10° × 10° at the equator) of sinusoidal projection; 16 such tiles cover the Amazon region (approximately 10°N–20°S, 80°–45°W). The data were obtained from the NASA Land Processes Data Active Archive Center (LP DAAC) (USGS 2011a) for the period February 2000–December 2009. A previous version of EVI data, collection 4 (C4), was also used in this study, although this dataset is now decommissioned and deleted from the NASA LP DAAC archives [the July–September (JAS) C4 *Terra* MODIS EVI data but not the corresponding quality flags for the years 2000–05 were obtained from Saleska et al. (2007)]. We have also used two other datasets. First, we used the vegetation indices monthly L3 global 0.05deg CMG (MOD13C2) dataset, which contains EVI at 0.05° × 0.05° spatial resolution and a monthly frequency. Second, we used the vegetation indices 16-day L3 global 0.05deg CMG (MOD13C1) dataset, which contains EVI at 0.05° × 0.05° spatial resolution and a 16-day frequency. These are cloud-free spatial composites of MOD13A2 (USGS 2011b). These were obtained from the NASA LP DAAC (USGS 2011b) for the period February 2000–December 2009. We also were able to obtain C4 MOD13C1 data with quality flags for 2004–06 (USGS 2011b).

2.2. Land-cover data

Land-cover information was obtained from the MODIS *Terra* land cover type yearly L3 global 1 km SIN grid product (MOD12Q1). This is the official NASA C5 land-cover dataset (USGS 2011c; Friedl et al. 2010). It consists of five land-cover classification schemes at 0.5 km × 0.5 km spatial resolution. The International Geosphere Biosphere Programme (IGBP) land-cover classification scheme was used to identify forest pixels in the Amazon region.

2.3. Aerosol data

Daily aerosol optical thickness (AOT) was obtained from the level 3 daily joint aerosol/water vapor/cloud product (MOD08_D3) at 1° × 1° spatial resolution. These were obtained from the NASA Level 1 and Atmosphere Archive and

Distribution System (LAADS) (NASA 2011a) for the months of July–September of the years 2000–06. We used the optical_depth_land_and_ocean_mean_mean data field from this product, which contains AOT at 550 nm. Similarly, monthly AOT was obtained from the level 3 monthly joint aerosol/water vapor/cloud product (MOD08_M3) at 1° × 1° spatial resolution. We used the corrected_optical_depth_land_QA_mean data field from this product, which contains AOT at 550 nm.

3. Methods

VI products are generated from surface reflectance data that have undergone atmospheric correction. However, residual atmospheric effects that remain in these data can be assessed by using 16-bit quality flags in both 1 km × 1 km as well as the 0.05° × 0.05° VI products. Sets of bits, from these 16 bits, are assigned to flags pertaining to clouds and aerosols, as well as flags that provide aggregate measures of data quality called VI usefulness indices, as detailed below.

Cloud quality flags are single bit (binary) flags indicating the presence (1) or absence (0) of clouds. In MOD13A2, each 1 km × 1 km 16-day VI composite value is accompanied by three binary cloud quality flags: adjacent cloud detected (bit 8), mixed clouds (bit 10), and possible shadows (bit 15). In the case of MOD13C1/C2, each 0.05° × 0.05° monthly EVI value has two binary cloud quality flags: adjacent cloud detected (bit 8) and mixed clouds (bit 10).

Aerosol quality flag, 2 bits in precision, provides information on aerosol content and is named aerosol quantity. It occupies the same bit positions, bits 6 through 7, in both MOD13A2 and MOD13C1/C2. The aerosol quality flag can assume one of four values: climatology (00), low (01), average (10), and high (11). The low, average, and high values refer to aerosol optical depth (AOT) at 550 nm less than 0.2, between 0.2 and 0.5, and greater than 0.5, respectively (Vermote and Vermuelen 1999). On the other hand, the climatology value indicates that the actual AOT is unknown, most likely because of presence of clouds, and climatological (long-term average) AOT is used in the process of atmospheric correction (Vermote and Vermuelen 1999).

The VI usefulness flag, 4 bits in precision, provides an aggregate measure of EVI quality. It occupies the same bit positions, bits 2 through 5, in both MOD13A2 and MOD13C1/C2 and can assume values from 0 (0000: best quality) to 15 (1111: not useful).

4. Results and discussion

Remote sensing of the Amazon forests at solar wavelengths is complicated due to persistent cloud and aerosols presence. Atmospheric corruption of surface reflectance data, from which the vegetation indices are evaluated, depends on prevailing cloud and aerosol optical thicknesses, among other factors (Vermote and Kotchenova 2008; Tanre et al. 1992). The two data quality indicators, quality flags and VI usefulness indices, accompanying the VI data indicate extensive cloud and aerosol corruption over the entire Amazon region (Figures 1a,b); about 81% of the forest pixels have at least one of the six 16-day VI composites in the third quarter of 2005 corrupted with clouds or aerosols and 56% have two or more composites

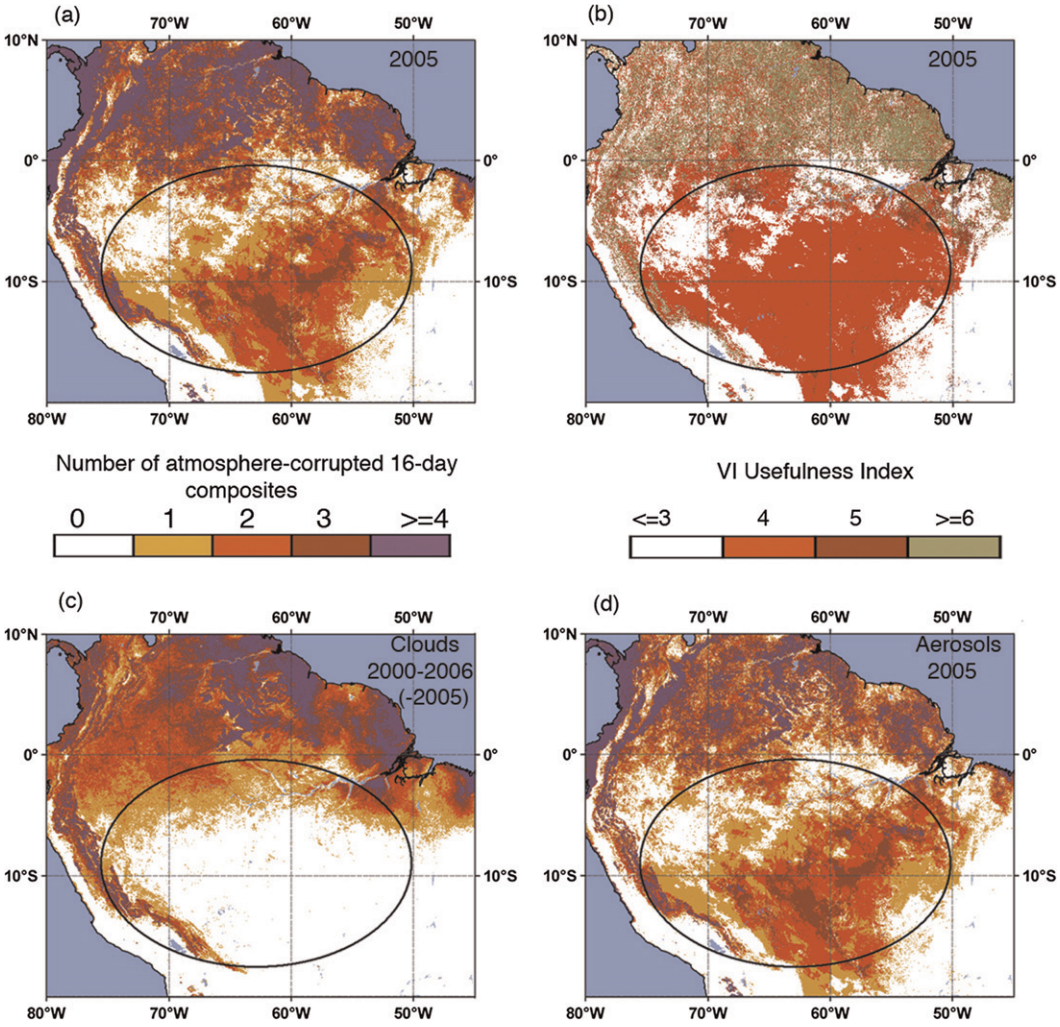

Figure 1. Spatial patterns of atmosphere corruption of C5 VI (1 km × 1 km) data during the JAS quarter. (a) Number of 16-day VI composites in the JAS quarter of 2005 with quality flags indicating cloud (adjacent cloud, mixed clouds, and possible shadow) or aerosol (climatology and high aerosols) corruption. (b) VI usefulness index values corresponding to (a). When a VI value is atmosphere corrupted only once, the corresponding VI usefulness index is its VI usefulness index value. When a pixel is atmosphere corrupted twice or more, the corresponding index is the mode of the VI usefulness index values. When a pixel is not atmosphere corrupted even once, the corresponding index is the mode of all six VI usefulness index values. (c) Average number of 16-day VI composites in the JAS quarter of 2000–06 (excluding 2005) with quality flags indicating clouds (adjacent cloud, mixed clouds, and possible shadow). (d) As in (c), but with quality flags indicating aerosols (climatology and high aerosols). The ellipse in each panel denotes the dominant drought-affected region during JAS 2005.

similarly corrupted. Cloud and aerosol presence and their radiation scattering properties are highly dynamic, both spatially and temporally; nevertheless, it is instructive to look at some summary statistics relevant to this study.

Clouds are especially pervasive north of the equator during the July–September quarter; here, on average, 90% of the pixels have two or more of the six 16-day dry season VI composites corrupted with clouds or their shadows (Figure 1c). This corruption is only somewhat less, 75%, in 2005 (figure not shown for brevity). South of the equator, cloud contamination is much less extensive—on average about 22%—because it is dry season here and even lesser during 2005 because of the drought (9%). Within the drought-stricken region itself, not surprisingly, only about 6% of the pixels exhibit cloud contamination during the third quarter of 2005.

Aerosol presence is more extensive in the Amazon during the dry season because of biomass burning (Eck et al. 1998; Schafer et al. 2002a; Schafer et al. 2002b; Artaxo et al. 1998; Artaxo et al. 2002). About 74% of the pixels north of the equator had two or more of the six 16-day VI composites during July–September 2005 corrupted due to failure of the aerosol retrieval algorithm because of cloudiness and subsequent use of climatological aerosol amount for atmospheric correction (Figure 1d); the average number is even higher, 86%, based on data from other years (2000–06; see Figure S2 of Samanta et al. 2010). South of the equator in the drought-stricken region, the respective numbers are 36% for 2005 and 19% for other years, but the corruption here is due to high aerosol amount, especially during the months of August and September (Samanta et al. 2010). These numbers may appear low, but that is misleading, because different pixels show aerosol corruption at different times and, as a result, few pixels within the study region actually have the full complement of uncorrupted time series data required for an unbiased analysis.

The spatiotemporal evolution of aerosol amount during the 2005 dry season is apparent from Figure 2: aerosol optical depths in excess of 0.5 at 550 nm begin to appear during the first half of August in the southern Amazon, covering nearly the entire drought-stricken region, and over the next 45 days the aerosol loads grow rapidly, reaching values of 1 and above, which are anomalously high when compared to other years during the period 2000–06, as noted by Koren et al. (Koren et al. 2007) and Bevan et al. (Bevan et al. 2009). In the drought-affected region, 82%, 58%, and 84% of the pixels have AOT values greater than 0.5 during the last three 16-day compositing periods in the third quarter of 2005 (Figures 2d–f); conservatively speaking, over 80% of the drought-affected region was under a thick haze for 40% of the time during the third quarter of 2005. This threshold AOT value of 0.5 at 550 nm is generally taken as the limit beyond which the corresponding surface reflectance data, hence VI, are deemed not useful for remote sensing of vegetation (NASA 2011b; MODIS 2011; Didan and Huete 2006; Vermote and Kotchenova 2008). The fact that the spatiotemporal patterns of AOT magnitudes change from year to year (Koren et al. 2007; Bevan et al. 2009) invalidates any arguments regarding the validity of differences in corrupted EVI values between years as indicative of actual greenness changes (as in Saleska et al. 2007).

It is instructive to contrast the actual day-to-day variation in AOT over the drought-affected region during 2005 with other years, as in Figure 3. Starting from

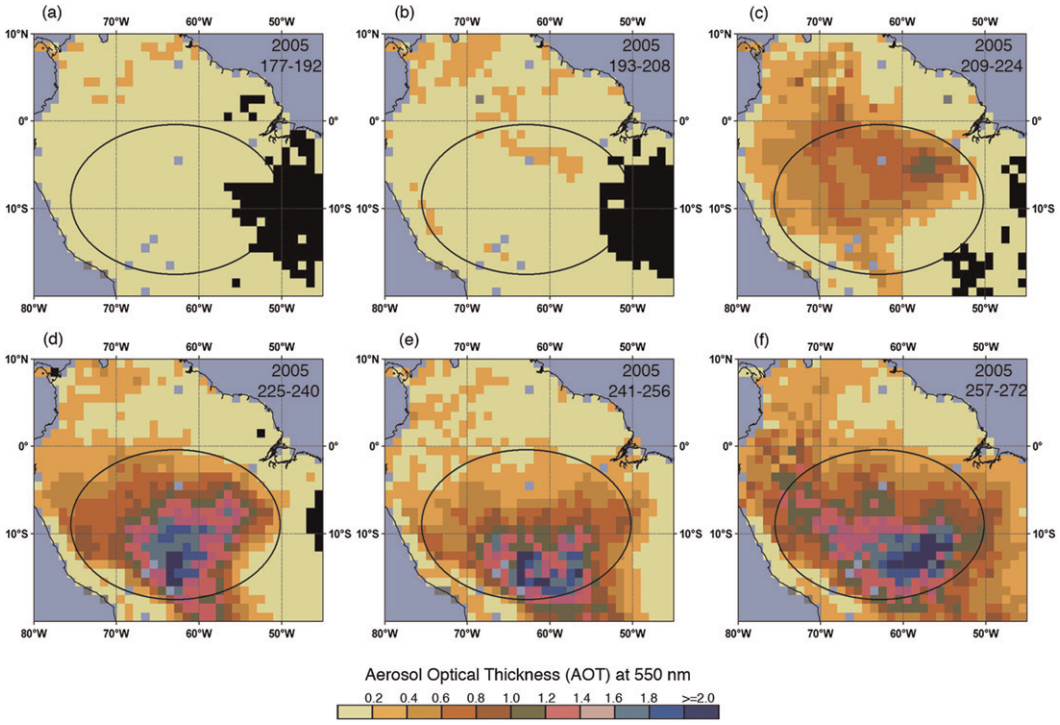

Figure 2. Spatial patterns of MODIS AOT at 550 nm, at 1° × 1° spatial resolution, during the dry season (JAS) of 2005. Shown here are patterns of mean AOT over the 16-day period corresponding to each of the six 16-day EVI composites covering JAS 2005. Negative AOT values are colored black. The ellipse in each panel denotes the dominant drought-affected region during JAS 2005.

about day 216 (early August), AOT remains much greater than 0.5 throughout the entire 2005 dry season, rendering accurate atmospheric correction of MODIS measurements impossible. Compared to other years, the 2005 dry season was indeed extremely hazy, due in large part to a very high number of biomass fires reported (Aragao et al. 2007). By examining the date stamp of each pixel in the drought-affected region, we find that nearly 100% of the VI values during the second half of August and most of September were aerosol corrupted (Figure 3). This renders any analysis of VI data in this region at 16-day scale fraught with biases. Even at monthly scale, we find that nearly 60%–66% of the drought-stricken region has insufficient valid VI data, which makes it difficult to draw any conclusions on the greenness dynamics of Amazon forests because of cloud and aerosol corruption.

Atmospheric corruption of is known to artificially reduce NDVI values (e.g., Holben 1986; Huete et al. 2002). The EVI was designed to improve upon NDVI by introducing aerosol resistance (Huete et al. 2002): that is, mitigate aerosol effects by using the blue band to correct for aerosol influence in the red band (Kaufman and Tanre 1992). This raises an important question: how do residual aerosol effects (given that the input surface reflectance data were generated after

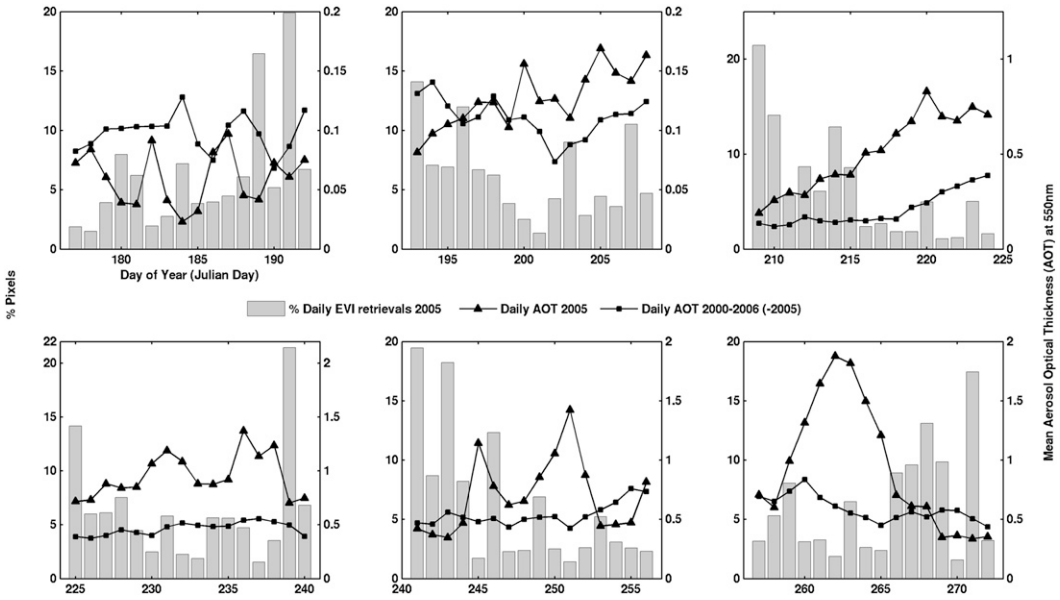

Figure 3. Distribution (percent of pixels) of daily C5 VI (1 km × 1 km) retrievals in intact forests in the drought-affected area south of the equator for all six 16-day VI composites during JAS 2005 (left axis). Daily MODIS AOT averaged over the same region (right axis) for JAS 2005 (in red) and 2000–06 (excluding 2005, in black).

atmospheric correction) impact magnitudes of C4 and C5 EVI data? To identify corrupted and uncorrupted pixels, we used C5 data quality filters, which superseded C4 filters, for both C4 and C5 EVI data (cf. section 3). This allowed an accurate assessment of atmosphere-corruption effects on EVI across collections by not introducing errors related to changes in data filters between collections. This is further justified by a high degree of similarity in cloud and aerosol flags between C4 and C5 data reported in Samanta et al. (Samanta et al. 2011b). The difference in uncorrupted EVI values between C4 and C5 is, as to be expected, negligible (0.02 or less compared to an average EVI value of 0.5), both during the dry season of 2005 (Figure 4a) and in other years as well (results not shown for brevity). Interestingly, the difference between corrupted and uncorrupted C5 EVI values is small (Figure 4b), which must be due to refinements to atmospheric correction (Vermote and Kotchenova 2008) and EVI algorithms (Didan and Huete 2006), because the difference between these two classes of pixels in C4 is quite large: corrupted EVI values are greater than uncorrupted values by 0.1 and more, especially in areas of high aerosol amounts (cf. Figures 1d, 4c). Aside from the large difference, the sign of this change is counterintuitive, because atmospheric corruption decreases estimates of vegetation greenness (Holben 1986; van Leeuwen et al. 2006), which is the reason for maximum-value compositing of vegetation index data: that is, selecting the largest vegetation index value among a set of daily values to represent a compositing period (16 days in the case of MODIS EVI). This suggests unusual behavior of the C4 EVI algorithm in the face of residual

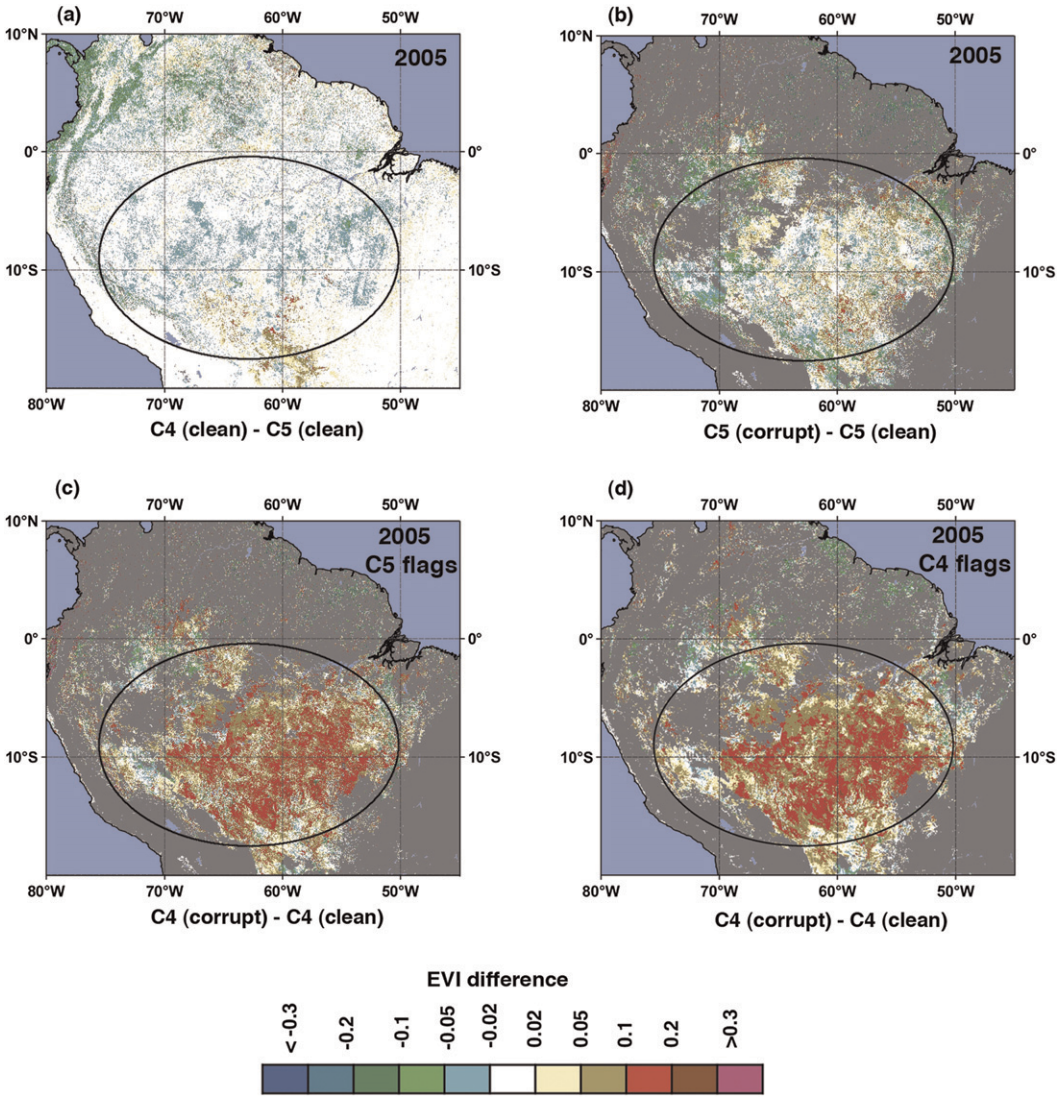

Figure 4. Spatial patterns of EVI differences during the 2005 dry season (JAS) at 1 km × 1 km spatial resolution. (a) Difference between uncorrupted C4 and C5 EVI values. (b) Difference between corrupted and uncorrupted C5 EVI values. (c) Difference between corrupted and uncorrupted C4 EVI values. (d) As in (c), but using C4 flags (0.05° × 0.05° spatial resolution). A 16-day composite EVI value is deemed corrupt if the aerosol-quantity quality flag indicates high aerosols. Likewise, a 16-day composite EVI value is deemed uncorrupted if the aerosol-quantity quality flag does not indicate high aerosols. In all cases, cloud contamination (mixed clouds, adjacent clouds, and shadows) is absent. The ellipse in the panels shows the drought-affected region.

atmospheric effects in surface reflectance data, from which the EVI is evaluated but has been fixed in the C5 algorithm. This behavior, as explained below, would result in artificially enhanced greening of vegetation when atmosphere-corrupted data are included in the analysis.

When surface reflectance data have (residual) aerosol corruption, as in C4 data, the resulting EVI values tend to be artificially inflated. This artifact can be traced to the EVI formulation; at a given near-infrared reflectance value, EVI decreases when red and blue reflectance values increase simultaneously, which correctly denotes increased obscuration of the surface under thicker atmospheres (Figure 5a). On the other hand, if only blue reflectance value increases [i.e., the ratio of blue to red reflectance (at given red reflectance) increases], EVI increases dramatically (Figure 5). Atmospheric effect at blue is much greater than at red, because scattering of solar radiation in the atmosphere increases nonlinearly with decrease in wavelength; this can easily result in blue band reflectance being greater than red band reflectance in situations of high aerosol loads, which will result in spuriously high values of EVI. Moreover, EVI will also increase if near-infrared reflectance increases as a result of incomplete atmospheric correction. These effects are demonstrated very well in C4 reflectance data (Figures 5c,d). Besides, inconsistency between multisensor EVI arising from problematic blue band reflectance values was noted in Fensholt et al. (Fensholt et al. 2006). The fact that such large differences between corrupted and uncorrupted EVI values are not seen in C5 (cf. Figures 4c,d vs. Figure 4b) could be due to better estimation of aerosol amount, thus affording more accurate atmospheric correction of MODIS measurements (Vermote and Kotchenova 2008), and to C5 EVI algorithm refinements (Didan and Huete 2006).

5. Conclusions

Cloud and aerosol corruption of satellite-based estimates of vegetation greenness is pervasive in the Amazon; nearly the entire region lacks a sufficient number of uncorrupted observations during the months of October–March. Even in the dry season (e.g., July–September 2005), about 81% of the forest pixels have at least one of the six 16-day VI composites corrupted with clouds or aerosols and 56% have two or more composites similarly corrupted. Under these conditions, spectrally varying residual atmospheric effects in surface reflectance data introduce artifacts into greenness indices; the EVI is particularly susceptible to such artifacts given its formulation and use of blue channel surface reflectance data. Such artifacts due to aerosol corruption—large patches of enhanced greenness—are especially obvious in collection 4 EVI data.

This analysis does not imply that satellite-measured greenness data are completely ineffective for studying vegetation changes in the Amazon but rather demonstrates that there is a need to rigorously evaluate these greenness data, as appropriate to a given application. For instance, future research should investigate how such greenness data could be validated against, as well as used synergistically with, data from other sources. These sources include other satellite sensors with different spatial, temporal, and spectral band characteristics (multispectral, hyperspectral, radar, and microwave) and, importantly, data from field measurements. Further, the impact of future improvements in atmospheric correction algorithms

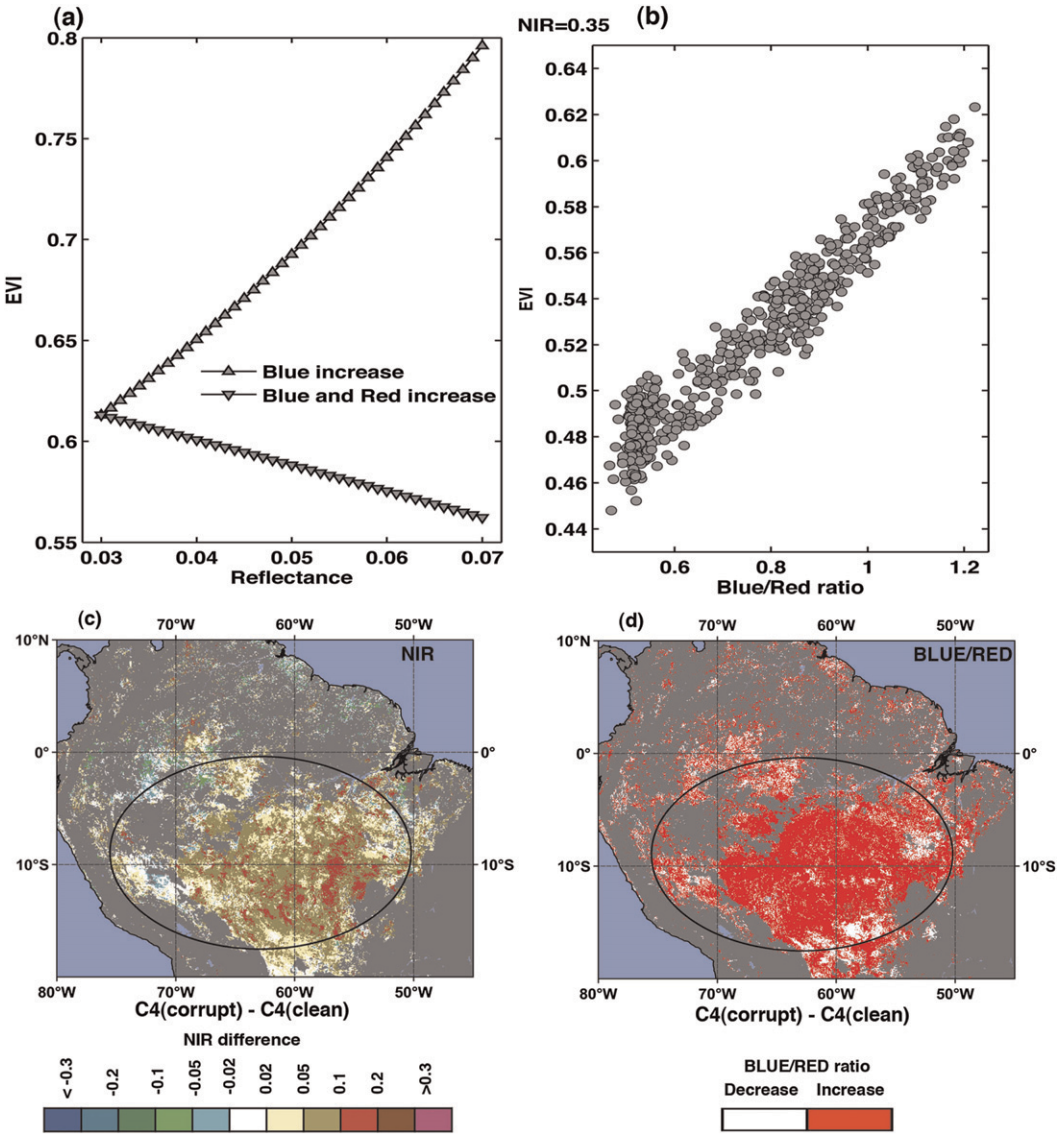

Figure 5. Sensitivity of EVI to blue band reflectance. (a) Theoretical calculations showing changes in EVI when only blue band reflectance increases (red) and when both blue and red band reflectances increase (green). NIR band reflectance is fixed at 0.35 in these calculations. (b) C5 (0.05° × 0.05°) EVI vs blue to red reflectance ratio in Amazon forests during JAS 2005. The blue to red ratios shown here are estimated from blue band reflectance values varying from 0.029 to 0.084 and a narrow interval of red band reflectance (0.06–0.07). NIR reflectance varied between 0.34 and 0.36. (c) Spatial patterns of C4 NIR reflectance differences between corrupted and uncorrupted, using C4 flags, during the 2005 dry season (JAS) at 0.05° × 0.05° spatial resolution. (d) As in (c), but for blue to red reflectance ratio.

(e.g., collection 6 and beyond) on the effectiveness of greenness data should be studied. Finally, there is a need to understand what other regions in the world show similar issues.

Acknowledgments. This research was funded by the NASA Earth Science Enterprise.

References

Aragao, L., Y. Malhi, R. M. Roman-Cuesta, S. Saatchi, L. O. Anderson, and Y. E. Shimabukuro, 2007: Spatial patterns and fire response of recent Amazonian droughts. *Geophys. Res. Lett.,* **34,** L07701, doi:10.1029/2006GL028946.

Artaxo, P., E. T. Fernandes, J. V. Martins, M. A. Yamasoe, P. V. Hobbs, W. Maenhaut, K. M. Longo, and A. Castanho, 1998: Large-scale aerosol source apportionment in Amazonia. *J. Geophys. Res.,* **103** (D24), 31 837–31 847.

——, and Coauthors, 2002: Physical and chemical properties of aerosols in the wet and dry seasons in Rondonia, Amazonia. *J. Geophys. Res.,* **107,** 8081, doi:10.1029/2001JD000666.

Asner, G. P., A. R. Townsend, and B. H. Braswell, 2000: Satellite observation of El Nino effects on Amazon forest phenology and productivity. *Geophys. Res. Lett.,* **27,** 981–984.

Bevan, S. L., P. R. J. North, W. M. F. Grey, S. O. Los, and S. E. Plummer, 2009: Impact of atmospheric aerosol from biomass burning on Amazon dry-season drought. *J. Geophys. Res.,* **114,** D09204, doi:10.1029/2008JD011112.

Dessay, N., H. Laurent, L. A. T. Machado, Y. E. Shimabukuro, G. T. Batista, A. Diedhiou, and J. Ronchail, 2004: Comparative study of the 1982-1983 and 1997-1998 El Nino events over different types of vegetation in South America. *Int. J. Remote Sens.,* **25,** 4063–4077.

Didan, K., and A. R. Huete, 2006: MODIS vegetation index product series collection 5 change summary. 17 pp. [Available online at http://landweb.nascom.nasa.gov/QA_WWW/forPage/MOD13_VI_C5_Changes_Document_06_28_06.pdf.]

Eck, T. F., B. N. Holben, I. Slutsker, and A. Setzer, 1998: Measurements of irradiance attenuation and estimation of aerosol single scattering albedo for biomass burning aerosols in Amazonia. *J. Geophys. Res.,* **103** (D24), 31 865–31 878.

Fensholt, R., I. Sandholt, and S. Stisen, 2006: Evaluating MODIS, MERIS, and VEGETATION—Vegetation indices using in situ measurements in a semiarid environment. *IEEE Trans. Geosci. Remote Sens.,* **44,** 1774–1786.

Ferreira, L. G., and A. R. Huete, 2004: Assessing the seasonal dynamics of the Brazilian Cerrado vegetation through the use of spectral vegetation indices. *Int. J. Remote Sens.,* **25,** 1837–1860.

Friedl, M. A., D. Sulla-Menashe, B. Tan, A. Schneider, N. Ramankutty, A. Sibley, and X. M. Huang, 2010: MODIS collection 5 global land cover: Algorithm refinements and characterization of new datasets. *Remote Sens. Environ.,* **114,** 168–182.

Gurgel, H. C., and N. J. Ferreira, 2003: Annual and interannual variability of NDVI in Brazil and its connections with climate. *Int. J. Remote Sens.,* **24,** 3595–3609.

Holben, B. N., 1986: Characteristics of maximum-value composite images from temporal AVHRR data. *Int. J. Remote Sens.,* **7,** 1417–1434.

Huete, A., K. Didan, T. Miura, E. P. Rodriguez, X. Gao, and L. G. Ferreira, 2002: Overview of the radiometric and biophysical performance of the MODIS vegetation indices. *Remote Sens. Environ.,* **83** (1–2), 195–213.

——, and Coauthors, 2006: Amazon rainforests green-up with sunlight in dry season. *Geophys. Res. Lett.,* **33,** L06405, doi:10.1029/2005GL025583.

Justice, C. O., and Coauthors, 1998: The Moderate Resolution Imaging Spectroradiometer (MODIS): Land remote sensing for global change research. *IEEE Trans. Geosci. Remote Sens.,* **36,** 1228–1249.

Kaufman, Y. J., and D. Tanre, 1992: Atmospherically resistant vegetation index (ARVI) for EOS-MODIS. *IEEE Trans. Geosci. Remote Sens.,* **30,** 261–270.

Koren, I., L. A. Remer, and K. Longo, 2007: Reversal of trend of biomass burning in the Amazon. *Geophys. Res. Lett.,* **34,** L20404, doi:10.1029/2007GL031530.

MODIS, cited 2011: Validation status. MODIS Land Surface Reflectance Science Computing Facility. [Available online at http://modis-sr.ltdri.org/validation/accuracy_uncertainty.html.]

Myneni, R. B., F. G. Hall, P. J. Sellers, and A. L. Marshak, 1995: The interpretation of spectral vegetation indexes. *IEEE Trans. Geosci. Remote Sens.,* **33,** 481–486.

——, and Coauthors, 2007: Large seasonal swings in leaf area of Amazon rainforests. *Proc. Natl. Acad. Sci. USA,* **104,** 4820–4823.

NASA, cited 2011a: LAADS web. NASA Level 1 and Atmosphere Archive and Distribution System. [Available online at http://ladsweb.nascom.nasa.gov/.]

——, cited 2011b: Product quality documentation for MOD13A2, C5. [Available online at http://landweb.nascom.nasa.gov/cgi-bin/QA_WWW/detailInfo.cgi?prod_id=MOD13A2&ver=C5.]

Rahman, A. F., D. A. Sims, V. D. Cordova, and B. Z. El-Masri, 2005: Potential of MODIS EVI and surface temperature for directly estimating per-pixel ecosystem C fluxes. *Geophys. Res. Lett.,* **32,** L19404, doi:10.1029/2005GL024127.

Saleska, S. R., K. Didan, A. R. Huete, and H. R. da Rocha, 2007: Amazon forests green-up during 2005 drought. *Science,* **318,** 612–612.

Samanta, A., S. Ganguly, H. Hashimoto, S. Devadiga, E. Vermote, Y. Knyazikhin, R. R. Nemani, and R. B. Myneni, 2010: Amazon forests did not green-up during the 2005 drought. *Geophys. Res. Lett.,* **37,** L05401, doi:10.1029/2009GL042154.

——, M. H. Costa, E. L. Nunes, S. L. Vieira, L. Xu, and R. Myneni, 2011a: Comment on ‘‘Drought-induced reduction in global terrestrial net primary production from 2000 through 2009.’’ *Science,* **333,** 1093, doi:10.1126/science.1199048.

——, S. Ganguly, and R. B. Myneni, 2011b: MODIS enhanced vegetation index data do not show greening of Amazon forests during the 2005 drought. *New Phytol.,* **189,** 12–15.

——, and Coauthors, 2012: Seasonal changes in leaf area of Amazon forests from leaf flushing and abscission. *J. Geophys. Res.,* G01015, doi:10.1029/2011JG001818.

Schafer, J. S., B. N. Holben, T. F. Eck, M. A. Yamasoe, and P. Artaxo, 2002a: Atmospheric effects on insolation in the Brazilian Amazon: Observed modification of solar radiation by clouds and smoke and derived single scattering albedo of fire aerosols. *J. Geophys. Res.,* **107,** 8074, doi:10.1029/2001JD000428.

——, T. F. Eck, B. N. Holben, P. Artaxo, M. A. Yamasoe, and A. S. Procopio, 2002b: Observed reductions of total solar irradiance by biomass-burning aerosols in the Brazilian Amazon and Zambian Savanna. *Geophys. Res. Lett.,* **29,** 1823, doi:10.1029/2001GL014309.

Sims, D. A., and Coauthors, 2008: A new model of gross primary productivity for North American ecosystems based solely on the enhanced vegetation index and land surface temperature from MODIS. *Remote Sens. Environ.,* **112,** 1633–1646.

Tanre, D., B. N. Holben, and Y. J. Kaufman, 1992: Atmospheric correction algorithm for NOAA-AVHRR products—Theory and application. *IEEE Trans. Geosci. Remote Sens.,* **30,** 231–248.

Tucker, C. J., 1979: Red and photographic infrared linear combinations for monitoring vegetation. *Remote Sens. Environ.,* **8,** 127–150.

USGS, cited 2011a: Vegetation indices 16-day L3 global 1km. NASA Land Processes Data Active Archive Center, MOD13A2. [Available online at https://lpdaac.usgs.gov/lpdaac/products/modis_products_table/vegetation_indices/16_day_l3_global_1km/mod13a2.]

——, cited 2011b: Vegetation indices monthly L3 global 0.05deg CMG. NASA Land Processes Data Active Archive Center, MOD13C2. [Available online at https://lpdaac.usgs.gov/lpdaac/products/modis_products_table/vegetation_indices/monthly_l3_global_0_05deg_cmg/mod13c2.]

——, cited 2011c: Land cover type yearly L3 global 1km SIN grid. NASA Land Processes Data Active Archive Center, MOD12Q1. [Available online at https://lpdaac.usgs.gov/lpdaac/products/modis_products_table/land_cover/yearly_l3_global_1km2/mod12q1.]

van Leeuwen, W. J. D., B. J. Orr, S. E. Marsh, and S. M. Herrmann, 2006: Multi-sensor NDVI data continuity: Uncertainties and implications for vegetation monitoring applications. *Remote Sens. Environ.,* **100,** 67–81.

Vermote, E. F., and A. Vermuelen, 1999: Atmospheric correction algorithm: spectral reflectances (MOD09). MODIS Algorithm Theoretical Basis Document, 107 pp. [Available online at http://modis.gsfc.nasa.gov/data/atbd/atbd_mod08.pdf.]

——, and S. Kotchenova, 2008: Atmospheric correction for the monitoring of land surfaces. *J. Geophys. Res.,* **113,** D23S90, doi:10.1029/2007JD009662.

——, N. Z. El Saleous, and C. O. Justice, 2002: Atmospheric correction of MODIS data in the visible to middle infrared: First results. *Remote Sens. Environ.,* **83** (1–2), 97–111.

Xiao, X. M., S. Hagen, Q. Y. Zhang, M. Keller, and B. Moore, 2006: Detecting leaf phenology of seasonally moist tropical forests in South America with multi-temporal MODIS images. *Remote Sens. Environ.,* **103,** 465–473.

Xu, L., A. Samanta, M. H. Costa, S. Ganguly, R. R. Nemani, and R. B. Myneni, 2011: Widespread decline in greenness of Amazonian vegetation due to the 2010 drought. *Geophys. Res. Lett.,* L07402, doi:10.1029/2011GL046824.